http://journal.uir.ac.id/index.php/JGEET

E-ISSN : 2541-5794
P-ISSN : 2503-216X

Journal of Geoscience,
Engineering, Environment, and Technology
Vol xx No xx 20xx

RESEARCH ARTICLE

Segmentation of the Active Fault on the Cirebon-Semarang Segments as Revealed by DEM-Derived Geomorphic Indices

Miftahul Jannah [1,*], Astyka Pamumpuni[1] , Imam Achmad Sadisun[1]

[1] *Geological Engineering, Institut Teknologi Bandung, Jl. Ganesha No. 10, Bandung 40132, Indonesia.*

* Corresponding author : mjmiftaaa@gmail.com
Tel.:+62 877-8849-4482
Received: Oct 1, 2016; Accepted: Nov 20, 2016.
DOI: 10.24273/jgeet.2016.1.2.001

Abstract

This research focuses on the segmentation and tectonic activity of the Baribis-Kendeng Fault across the Cirebon to Semarang segments, revealed through the analysis of geomorphic indices derived from Digital Elevation Models (DEM). Utilizing geomorphic indices such as the Hypsometric Integral (HI), Stream Length-Gradient Index (SL), and SL/K ratio, the analysis was conducted on 33 streams crossing ten segments. The results indicate that the landscape in the research area is predominantly in the youthful stage, with HI values ranging from 0.459 to 0.492, indicating active tectonic uplift. Segments such as Ungaran and Pemalang exhibit significant tectonic activity, with high SL/K values, particularly in the Ungaran segment, where the SL/K value reaches 344.872. These findings suggest that fault activity in the region is ongoing, with stronger uplift patterns observed at the western and eastern ends of the fault, while relatively lower activity is found in the central area. This research highlights the ongoin tectonic processes shaping the region's geomorphology and contributes to a better understanding of the active fault system in Java Island.

Keywords: DEMNas, Faults, Hypsometric Integral (HI), Stream Length Gradient Index (SL)

1. Introduction

The transition from oblique to frontal subduction between Sumatra and southern Java has resulted in distinct structural and seismic characteristics in these regions. Java generally exhibits lower seismic activity compared to Sumatra, although significant earthquakes and tsunamis hava also occurred in Java (Pusat Studi Gempa Nasional, 2017). Recent research has focused on mapping earthquake sources in Java, particularly active inland faults (Marliyani, 2016; Marliyani et al., 2016; Daryono, 2016; Supartoyo, 2016; Pusat Studi Gempa Nasional, 2017).

In recent decades, shallow inland earthquakes in Java have become more frequent, causing substantial damage due to the high population density (Pusat Studi Gempa Nasional, 2017). The extent of damage is influenced by both earthquake magnitude and local geological conditions (Daryono et al., 2009).

In recent times, the research of topographic and landforms using Digital Elevation Models (DEMs) and Geographic Information System (GIS) has provided a basis for the precise analysis of fault dynamics. DEMs are digital representations and simulations of the Earth's surface topography. The application of geospatial analysis and retrieval techniques from DEM data, encompassing streams, watersheds, and topographic features, has found extensive application in the fields of geomorphology, neotectonics, and active tectonics, especially when integrated with geological data (Radaideh and Mosar, 2019; Yu et al., 2020; Yang et al., 2022).

Active faults significantly contribute to earthquake occurances and can trigger various natural disasters (Hamzah et al, 2013; Yang et al., 2022). The Baribis-Kendeng fault system is a notable active fault associated with seismic activity in West and Central Java.

The physical attributes of streams are highly responsive to the geological dynamics within their watersheds, make them valuable indicators of tectonic processes. To address specific tectonic matters, parameters such as stream profiles, Hack profiles, stream length-gradient index (SL), normalized stream-gradient (SL/K), hypsometric integral (HI), and hypsometric curves are employed to assess tectonic deformation and erosion separately. This approach ensures a more precise analysis of how tectonic forces and erosional processes shape the landscape.

In this research, DEMNas is utilized to identify watersheds and streams intersecting active fault zones based on the PuSGeN 2017 catalog using MATLAB script and ArcGIS technology. The research involves extracting and calculating the stream profiles, Hack profiles, SL indexes, and the hypsometric integral (HI) values of the respective watersheds to measure fault activity across distinct fault segments.

2. Research Area

The research area is located in the northern coastal region of Java, administratively situated between Cirebon-Semarang. The selection area is based on a unique combination of geological, geographical, and tectonic factors. This region is known for significant tectonic activity, including active faults, folds, and other geological structures (Fig.1)

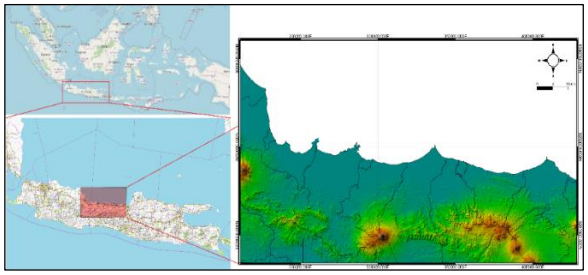

Fig 1. Research area location.

3. Active Fault Segments in Research Area

The streams studied (Table 1) cross the Baribis-Kendeng Fault in the Cirebon-Semarang segments (Fig. 2), which is an active geological structure in Java. This geological structure is predominantly characterized by strike-slip and thrust faults, with normal faults as minor features (Pusat Studi Gempa Nasional, 2017). The Baribis Fault in West Java, part of the back-arc imbrication, is identified as a thrust fault based on topography and seismic reflection data, and the frequently experiences seismic activity (Pusat Studi Gempa Nasional, 2017).

Table 1. Names of stream lines crossing the active fault on the research area.

Active Fault Segments	ID	Stream names	Stream length (km)
Cirebon-1	1	Ci Pakeleran	22.437
	2	Ci Keuyeup	8.749
	3	Ci Siluk	15.042
	4	Kali Pengasinan	4.732
	5	Kali Jaga	8.570
Cirebon	6	Ci Kanci	14.927
	7	Kali Canggah	6.915
	8	Ci Hambar	28.597
	9	Ci Juray	23.889
	10	Ci Lambu	6.215
Cirebon-2	11	Ci Panundaan	12.406
	12	Ci Beres	36.546
	13	Kali Kelampis	81.121
	14	Ci Jangkelok	38.660
Brebes	15	Kali Gurujugan	10.693
	16	Ci Caruy	38.676
	17	Kali Babakan	36.668
	18	Kali Bogor	14.621
	19	Kali Rambutan	25.700
Tegal	20	Kali Wuri	11.441
	21	Kali Kawung	8.505
	22	Kali Cenang	8.413
	23	Kali Semedo	12.050
Pemalang	24	Kali Waluh	52.537
	25	Kali Genjor	14.820
	26	Kali Comal	73.757
Pekalongan	27	Kali Paingen	54.858
	28	Kali Sengakarang	44.629
Weleri	29	Kali Kadunguling	4.325
	30	Kali Maron	7.389
Ungaran	31	Kali Blorong	47.897
Semarang	32	Kali Loning	9.978
	33	Kali Pakis	16.077

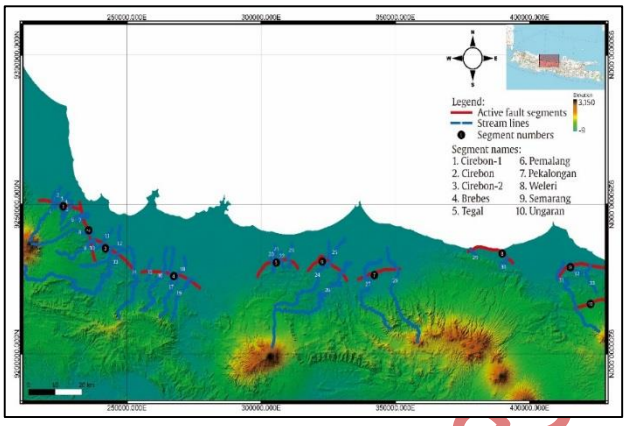

Fig 2. Active fault segments on research area.

The Kendeng Fault extends from Central to East Java, consisting of thrust faults and folds, ehich are evident through Bouguer anomalies (Hamilton, 1979; Simandjuntak & Barber, 1996; Smyth, 2008; Pusat Studi Gempa Nasional, 2017). The uplifted river terraces indicate active fault movement, with moderate earthquakes (M4-5) occurring along this fault zone (Marliyani, 2016). This fault is considered part of the Sundaland block boundary, along with the Baribis Fault (Koulali et al., 2016; Natawidjaja & Daryono, 2016).

The Semarang Fault is identified through the morphology of its fault scarp and seismic data. Historical seismic records show a significant earthquake in this region (Hidayat, 2013; Hidayat et al., 2011). Hidayat's (2013) research also indicated that the Kali Garang Fault is active and has the potential to trigger future earthquakes.

4. Regional Geology

The Cirebon-Semarang (Fig. 3) area is covered by the Geological Map Sheets of Arjawinangun (Djuri, 1995), Banjarnegara and Pekalongan (Chondon et al., 1996), Cirebon (Silitongan et al., 1996), Indramayu (Achdan and Sudana, 1992), Magelang-Semarang (Thanden et al., 1996), Majenang (Kastowo and Suwana, 1996), Purwokerto-Tegal (Djuri et al., 1996), and Tasikmalaya (Budhitrisna, 1986). This area features a complex and diverse geological framework influenced by tectonic, volcanic, and sedimentary process that have shaped the current rock formations and topography. The geology consists of igneous, sedimentary, and metamorphic rocks.

According to the geological map sheets, the western part of this area is dominated by volcanic rock formations such as andesite and basalt, resulting from volcanic activity. In the eastern part, near Semarang, sedimentary rock formations composed of alluvial deposits and sandstone are present, reflecting sedimentary processes from the Tertiary to the Quaternary. The northern part encompasses the northern coast of Java, characterized by alluvial deposits and sandstone formations, creating significant lowlands and river valleys. In the southern part, this area is marked by a chain of active volcanoes, including Cereme volcano, Slamet volcano, and Merapi volcano. These volcanoes produce volcanic rock formations such as andesite and basalt, along with pyroclastic deposits.

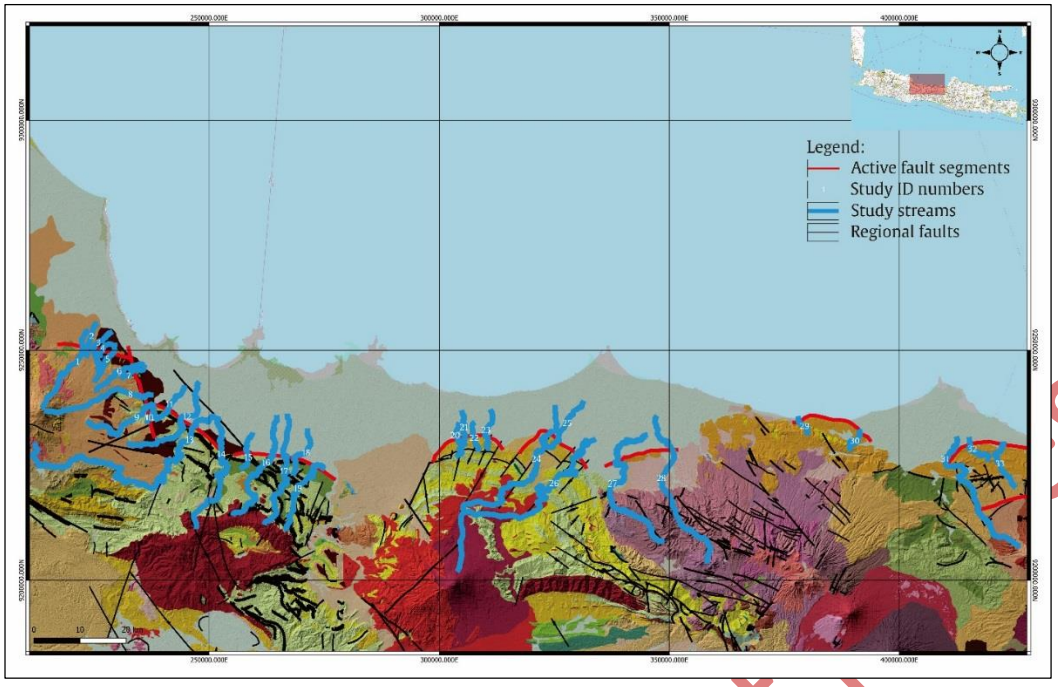

Fig 3. Digital Elevation Model (DEM) image overlaid with active fault segments (Pusat Studi Gempa Nasional, 2017) and regional geology (modified after Djuri, 1995; Chondon et al., 1996; Silitonga et al., 1996; Achdan and Sudana, 1992; Thanden et al., 1996; Kastowo and Suwarna,1996; Djuri et al., 1996; Budhitrisna, 1986).

3. Methods and Materials

The data used on this research is DEM data from DEMNas that downloaded from http://tides.big.go.id/DEMNAS/ ("DEMNAS, "n.d.). Based on the existing description, the spatial resolution of DEMNas is 0.27-second (arcsecond), equivalent to 8.2m using EGM2008 ("DEMNAS", n.d.) (Ekström dkk., 2012; QGIS Development Team, 2022; Pamumpuni et al., 2022). The data plotted and analyzed with QGIS 3.38 software.

The DEMNas data in the research area were analyzed utilizing MATLAB R2023a software to extract the stream network. Subsequently, this stream network was classified into 33 sub-basins to conduct morphometric analysis parameters in the research area. In order to assess active faults in the research area, the morphometric analysis encompassed longitudinal profile, hack profile, Hypsometric Integral (HI), Stream Length Gradient Index (SL) to interpret landscape changes from a tectono-geomorphological perspective. To date, such analysis has not been applied in the research area. The parameters were computed using QGIS and ArcGIS software. The overall methodology employed for this research is delineated in a flowchart (Fig. 4).

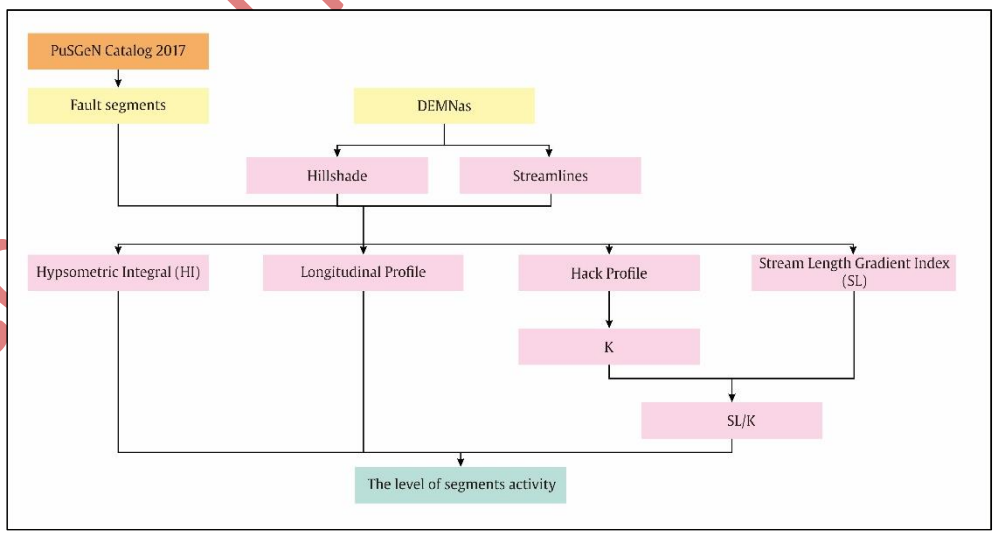

Fig 4. Illustrates a flow diagram detailing the methods used in the present investigation.

4. Morphometric Parameters

4.1 Extraction of River Systems

A stream system represents a landform shaped through the erosion, transportation, and deposition of surface water, often influenced by tectonic forces (Yang et al., 2022). In general, the surface and geomorphological features of specific regions are often determined by the level of neotectonic activity; specific tectonic movements mold particular geomorphological features and regulate the layout and configuration of the stream system (Zhang et al.,

2006). In this research, the extraction of the river system within the research area is conducted using the Matlab R2023a and QGIS technical platforms. The classification of river systems is based on the Strahler watershed system model (Strahler, 1952).

4.2 Stream Profile, Hack Profile, and Stream Length Index (SL)

The stream profile demonstrates a concave shape, with a level of concavity progressively increasing from the downstream to the upstream sections (Wheeler, 1979; see Fig. 5a). The general form of the stream profile is influenced by factors such as stream flow dynamics, particle size of the stream bed material, and sediment discharge within the stream (Snow and Slingerland, 1990). Variations in the stream profile at a local level are linked to the attributes of the stream bedrock, the influx of tributaries, and tectonic movements. Moreover, alterations in the stream's slope are discernible through its stream profile (Fig. 5c and d).

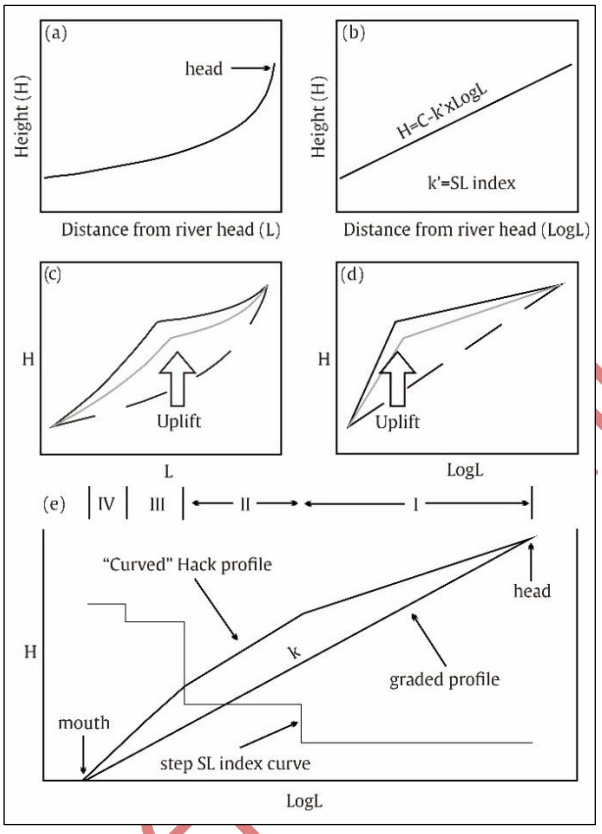

Fig 5. Conceptual diagrams of Hack profiles (after Chen et al., 2003). (a) The stream profile of a stream exhibiting graded conditions; (b) The semilogarithmic plot of a graded stream profile, the so-called Hack profile, is a straight line with a slope k', the SL index; (c) The uplifted longitudinal profile shows a distinct knickpoint with a steeper lower reach and; (d) its Hack profile; (e) A curved Hack profile may be divided into four graded segments (I, II, III, and IV), each of which is linearly fitted and has its own SL index construct the step curve (Chen et al., 2003).

To facilitate quantitative analysis of slope variations in streams, Hack (1973) introduced a parameter known as the stream length gradient index (SL index). The computation of the SL index is as follows:

$$SL = \frac{\Delta H}{\Delta L} . L \qquad (1)$$

In this equation, ΔH signifies the vertical change in elevation per unit length of the stream section, while L represents the distance from the headwater of the stream to the midpoint of the stream reach.

The SL value is highly responsive to changes in the slope of the stream bed. Within a watershed, a stream in equilibrium maintains a consistent SL value from its headwater to its mouth. Any sudden alteration in the SL value within a specific section of the stream is typically attributed to tectonic movements or variations in lithology. A notably high SL value indicates either a high resistance to erosion of the stream bed or placement of the stream reach in an uplifted area. Alternatively, a notably low SL value suggests either a low resistance to erosion of the bedrock or the placement of the stream reach in subsiding area (Zhao et al., 2014).

In addition, Hack (1973) found that the stream profile with similar erosion resistance can be expressed by a simple semilogarithmic equation:

$$H = c - k' \times \log(L) \qquad (1)$$

where H is the altitude of the profile, c is constant, and k' is the SL index. The quantity L is the stream length measured from the drainage divide at the source of the longest stream in the watershed. The semi-logarithmic plot of the longitudinal profile is hereafter called the Hack profile (Fig. 5b).

On a Hack profile, the straight line connecting the headwater of the river and the mouth of the watershed is called the graded profile, which represents the equilibrium state when the whole stream reaches dynamic equilibrium. The slope of this straight line is called the graded slope (K). Larger streams are more likely to have a larger K and SL index than smaller streams. Therefore, in order to compare the SL indexes among different streams, K should be used to normalize the SL index of different streams (Yang et al., 2022). Seeber and Gornitz (1983) divided the SL index of stream sections in the Himalayas by the K value of the stream in order to obtain the normalized stream gradient (SL/K). They proposed that a steep reach has a SL/K value between 2 and 10 and an extremely steep reach has a SL/K value greater than 10.

4.3 Hypsometric Integral (HI)

The hypsometric integral (HI) is a parameter used to characterize the distribution of elevation within a given area (Mayer, 1990). It holds significant geomorphological significance, providing insight into the developmental phase of streams (Keller and Pinter, 2002). There are two common calculation methods employed for determining the HI. A commonly employed method, proposed by Strahler (1952), offers a widely utilized mathematical model for assessing the developmental phase of erosional geomorphology, elucidating the interplay between stream geomorphology and erosion (Yang et al., 2022). This is the calculation of this method:

$$x = a/A \qquad (2)$$

$$y = h/H \qquad (3)$$

where a is the area above a contour in the basins, A is the whole watershed, h represents the difference in height between the highest contour and the outlet of the basin, and H represents the disparity in height between the highest point of the basin and its outlet. It's apparent that both the abscissa (x) and the ordinate (y) vary between 0 and 1. The HI value for a sequence of (x,y) data points is determined by the area enclosed between the curve and the coordinate axes (Fig. 6). This approach is employed to compute the HI value for the watersheds of 33 streams. An alternative method, proposed by Pike and Wilson (1971), determines the HI value through the following process:

$$HI = (H_{mean} - H_{min})/(H_{max} - H_{min}) \quad (4)$$

where H_{mean} represents the average elevation and (H_{max} – H_{min}) denotes the difference in elevation across the basin. These methods are utilized to compute the HI values within the research area.

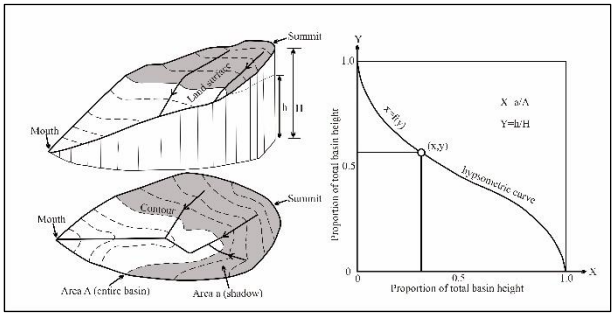

Fig 6. Schematic method of hypsometric index analysis (modified after Strahler, 1952 in Yang et al., 2022).

The HI values obtained from these methods offer insight into the geomorphic evolution phase of a watershed. According to Davis's theory of the geomorphic erosion cycle, as expounded by Strahler (1952), after a period of intense orogenic uplift, tectonic activity subsides, and surface geomorphic processes become predominantly governed by stream erosion. Consequently, it is anticipated that the HI value of the basin will progressively diminish over time.

In this research, it is used Jannah's (2024) classification to determine the categories of HI value. There are high (>0.44), moderate (0.34-0.44), and low (<0.34).

5. Results and Interpretation

5.1 Stream Profile, Hack Profile, and SL Index

The longitudinal profiles, Hack profiles, and SL indices for 33 streams traversing the Cirebon-Semarang segments were extracted using QGIS and MATLAB scripts (Fig. 7-16). The streams in this research range in length from 4 m to 80 km, with SL/K values ranging from 5 to 735. To facilitate comparison, SL/K values were divided into three quartiles. The values <245 are classified as relatively steep, values between 245-490 are classified as moderately steep, and values >490 are classified as very steep.

In the Cirebon-1 segment (Fig. 7), five watersheds were analyzed. The fault zone in this segment are located in the Young Volcanic Products of Cereme (Qyu) for Ci Pakeleran-Ci Suluk and the Gintung Formation (Qpg) for Kali Pengasingan-Kali Jaga. The longitudinal profiles show that Ci Keuyeup, Ci Siluk, and Kali Pengasinan exhibit steep elevation changes when crossing the fault zone, indicating uplift in the area. In contrast, watersheds Ci Pakeleran and Kali Jaga show elevation changes with gentler gradients, suggesting weaker or older fault activity. The Hack profiles for this segment reveal steep inclinations across all watersheds, indicating increased gradients due to tectonic uplift. The SL index results show that Ci Pakeleran has the highest value of 2825.437, indicating high tectonic activity. Ci Suluk and Kali Jaga have SL index values ranging from 274 to 357, suggesting moderate tectonic activity, while Kali Keuyeup and Kali Pengasinan have lower SL index values of 189 to 196, indicating lower tectonic activity.

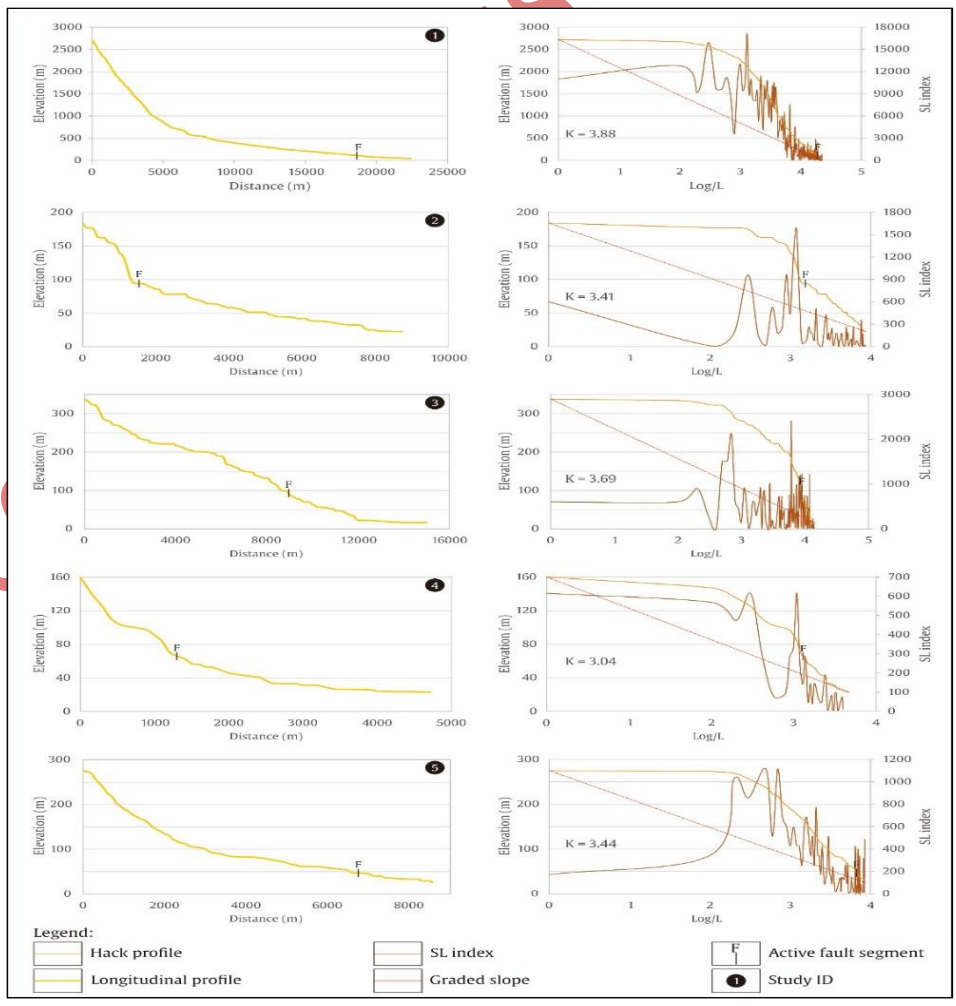

Fig. 7. Longitudinal profile, Hack profile, and SL indexes at Cirebon-1 segment.

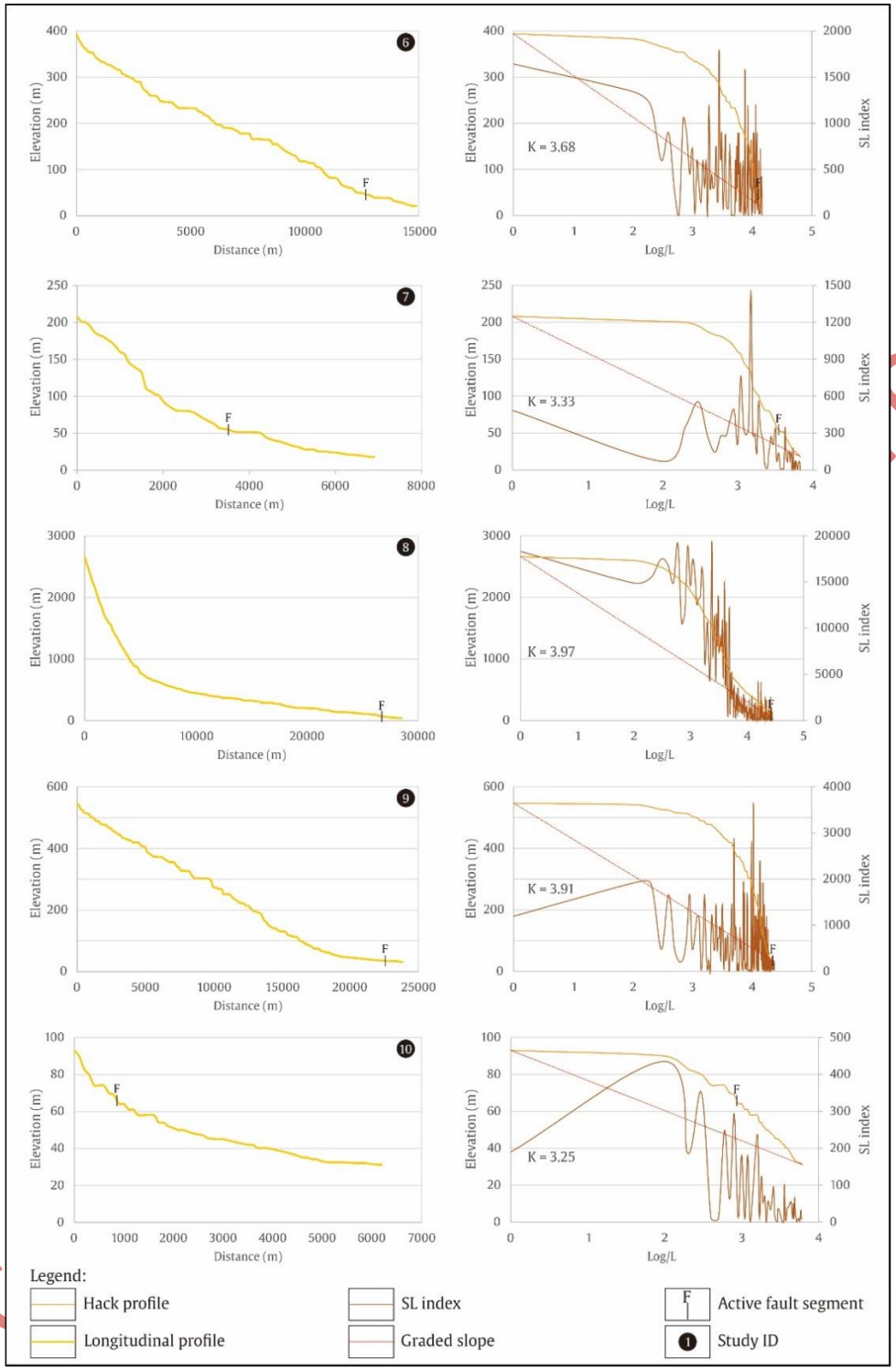

Fig. 8. Longitudinal profile, Hack profile, and SL indexes at Cirebon segment.

The Cirebon segment (Fig. 8) includes Ci Kanci to Ci Lambu. The fault zones in this segment are located in the Gintung Formation (Qpg) for watersheds Ci Kanci, Kali Canggah, and Ci Hambar, then Alluvial Deposits (Qa) for Ci Juray, and the Halang Formation (Tmph) for the Ci Lambu. Kali Canggah and Ci Lambu show uplift, as evidenced by slightly steep elevation changes across the fault zone. In contrast, Ci Kanci, Ci Hambar, and Ci Juray display gentler elevation changes, suggesting weaker or mor prolonged fault activity. The Hack profiles for this segment show that Ci Kanci has a steeper gradient compared to Kali Canggah to Ci Lambu, indicating a gradient increase due to tectonic uplift near the Cirebon-1 segment. Kali Canggah-Ci Lambu show slightly steeper gradients, though not as pronounced as in Ci Kanci. SL index analysis reveals that Ci Kanci has moderate tectonic activity with a SL index of 424.67. Watersheds 7 and 10 have lower SL index values of 72 to 198, indicating low tectonic activity, while Ci Hambar and Ci Juray exhibit high tectonic activity with SL index values ranging from 557 to 2920.

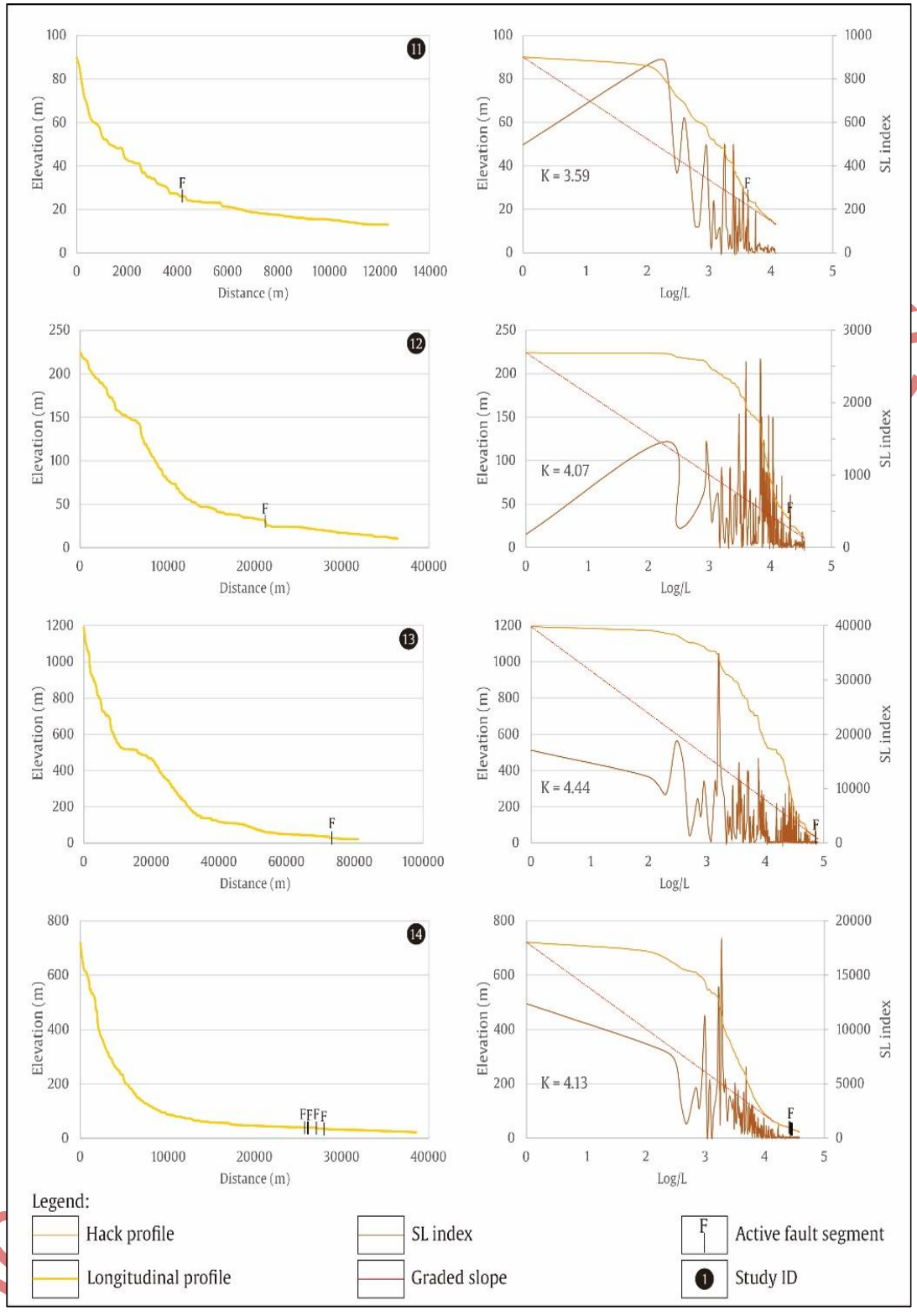

Fig. 9. Longitudinal profile, Hack profile, and SL indexes at Cirebon-2 segment.

In the Cirebon-2 segment (Fig. 9), four streams (Ci Panundaan to Ci Jangkelok) were analyzed. The fault zones are located in the Gintung Formation (Qpg) for Ci Panundaan, Alluvial Deposits (Qa) Ci Beres and Kali Kelampis, and a combination of Alluvial Deposits (Qa), Cijolang Formation (Tpcl), and Gintung Formation (Qpg) for Ci Jangkelok. These streams exhibit less pronounced elevation changes when crossing the fault zones. Ci Panundaan and Ci Beres show slight elevation changes, indicating minor uplift, while watersheds Kali Kelampisa and Ci Jangkelok show even gentler gradients due to lower tectonic activity. The Hack profiles indicate relatively steep gradients for Ci Panundaan-Ci Jangkelok, suggesting tectonic uplift. The SL indices vary, with high tectonic activity observed in Kali Kelampis and Ci Jangkelok with values ranging from 793 to 1383. Ci Beres shows moderate tectonic activity with a SL index of 263, while Ci Panundaan shows low tectonic activity with a SL index of 95.

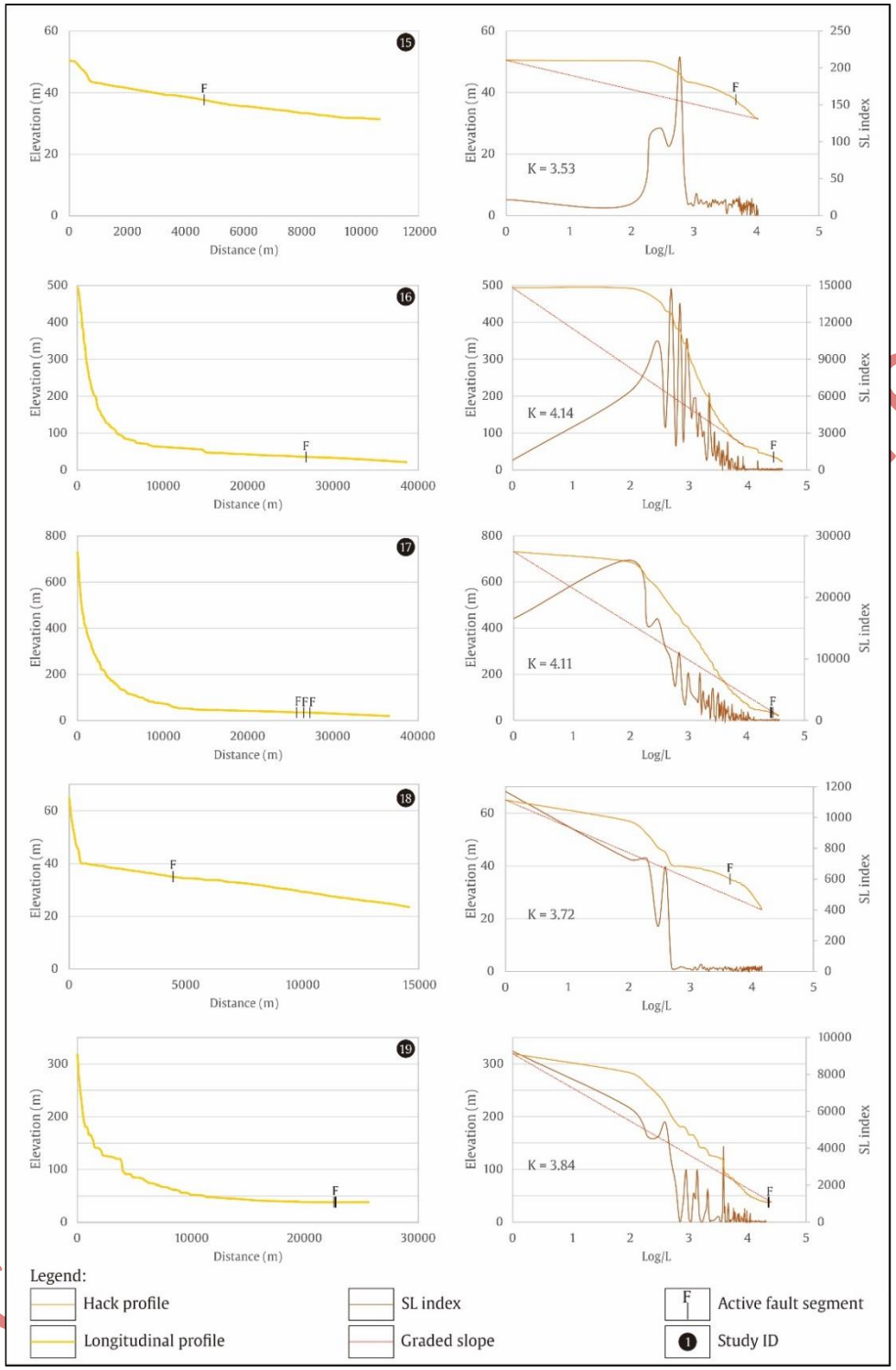

Fig. 10. Longitudinal profile, Hack profile, and SL indexes at Brebes segment.

The Brebes segment (Fig. 10) includes five streams (Kali Gurujugan-Kali Rambutan). The fault zones are located in the Halang Formation (Tmph) for Kali Gurujugan, Alluvial Deposits (Qa) for Ci Caruy and Kali Bogor, a combination of Halang Formation (Tmph) and Alluvial Deposits (Qa) for Kali Babakan, and Pemali Formation (Tmp) and Alluvial Deposits (Qa) for Kali Rambutan. The streams show gentle elevation changes in the Brebes segment, indicative of weak or long-standing fault activity. The Hack profiles reveal that only Kali Rambutan has a gentler gradient in this segment, while Kali Gurujugan to Kali Bogor show steeper inclinations, suggesting tectonic uplift due to regional structural influences. SL index values range from 20 to 818. Kali Gurujugan and Kali Bogor show low tectonic activity with SL indices of 20 to 44. Ci Caruy and Kali Babakan have high tectonic activity with SL indices ranging from 509 to 818. Kali Rambutan shows moderate tectonic activity with a SL index of 422.

The Tegal segment (Fig. 11) includes Kali Wuri to Kali Semedo. The fault zones are located in Alluvial Deposits (Qa) for Kali Wuri, Kali Kawung, and Kali Semedo, then in the Tapak Formation (Tpt) for Kali Cenang. The longitudinal

profiles show slightly steep elevation changes when crossing the fault zone, indicating uplift. The Hack profiles indicate that Kali Wuri, Kali Cenang, and Kali Semedo have steeper gradients compared to Kali Kawung, suggesting increased gradients due to tectonic uplift, while Kali Kawung shows relatively smaller uplift compared to the others. SL index values range from 60 to 180, indicating relatively low tectonic activity.

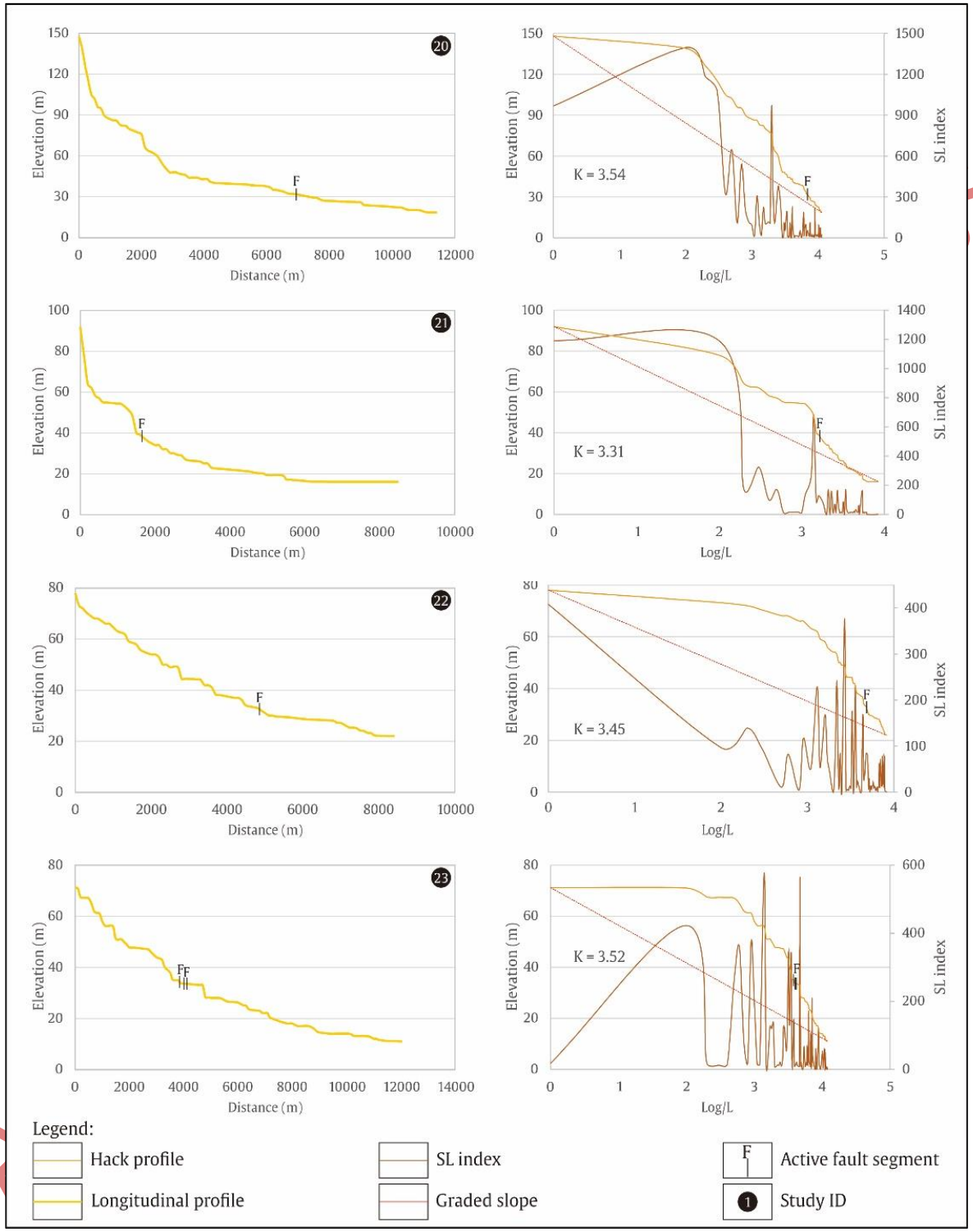

Fig. 11. Longitudinal profile, Hack profile, and SL indexes at Tegal segment.

In the Pemalang segment (Fig.12), Kali Waluh to Kali Comal were analyzed. The fault zone for Kali Waluh is located in the Undak Deposits (Qps), while for Kali Waluh and Kali Comal are in the Alluvial Deposits (Qa). The longitudinal profile for Kali Genjor shows slightly steep elevation changes, indicating minor uplift. Kali Waluh and Kali Comal show gentler gradients when crossing the fault zone, suggesting weaker or more prolonged fault activity. The Hack profiles indicate that Kali Waluh and Kali Genjor have relatively steep gradients, suggesting tectonic uplift, while Kali Comal has a gentler gradient, indicating less intense tectonic influence. SL index analysis shows high tectonic activity for Kali Waluh and Kali Comal with values ranging from 515 to 2477. Kali Genjor shows relatively low tectonic activity with a SL index of 48.

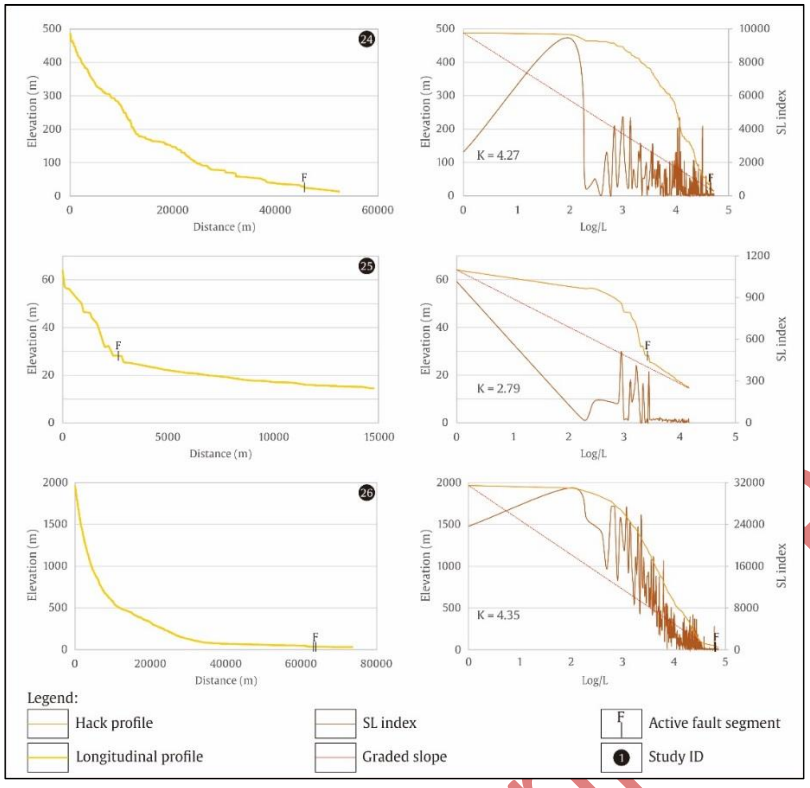

Fig. 12. Longitudinal profile, Hack profile, and SL indexes at Pemalang segment.

In the Pekalongan segment (Fig. 13), Kali Paingen and Kali Sengkarang were analyzed. The fault zones for these streams are located in Alluvial Deposits (Qa). Both streams exhibit similar elevation patterns with gentle gradients, indicating weak or prolonged fault activity. The Hack profiles also show similar patterns with gentle gradients. Despite this, there is a slight tectonic influence. The SL index indicates relatively high tectonic activity with values ranging from 1188 to 2072.

In the Weleri segment (Fig. 14), the fault zones are in Aluvium (Qf) for Kali Kadunguling and Alluvial Deposits (Qa) for Kali Maron. Both streams show similar elevation patterns with slightly steep gradients, indicating minor uplift. The Hack profiles reveal steep inclinations when crossing the fault zone. The SL index values range from 226 to 239, indicating moderate tectonic activity.

In the Ungaran segment (Fig. 15), Kali Blorong traverses the area with the fault zone located in the Kaligetas Formation (Qpkg). The stream shows relatively steep elevation changes when crossing the fault zone, indicating uplift. The Hack profile also shows steep gradients, reflecting increased tectonic activity. The SL index reveals high tectonic activity with a value of 1453.

Lastly, in the Semarang segment (Fig. 16), Kali Loning and Kali Pakis were analyzed. The fault zones are located in Alluvial Deposits (Qa). The longitudinal profiles show relatively gentle elevation changes, suggesting weak or prolonged fault activity. The Hack profiles indicate steep gradients, suggesting uplift. The SL index analysis reveals varying tectonic activity. Kali Loning shows low tectonic activity with a value of 115, while Kali Pakis shows moderate tectonic activity with value of 218.

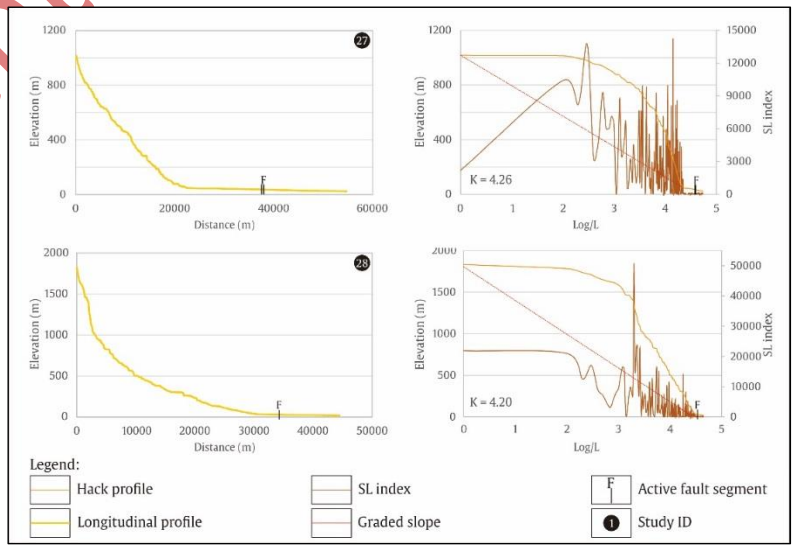

Fig. 13. Longitudinal profile, Hack profile, and SL indexes at Pekalongan segment.

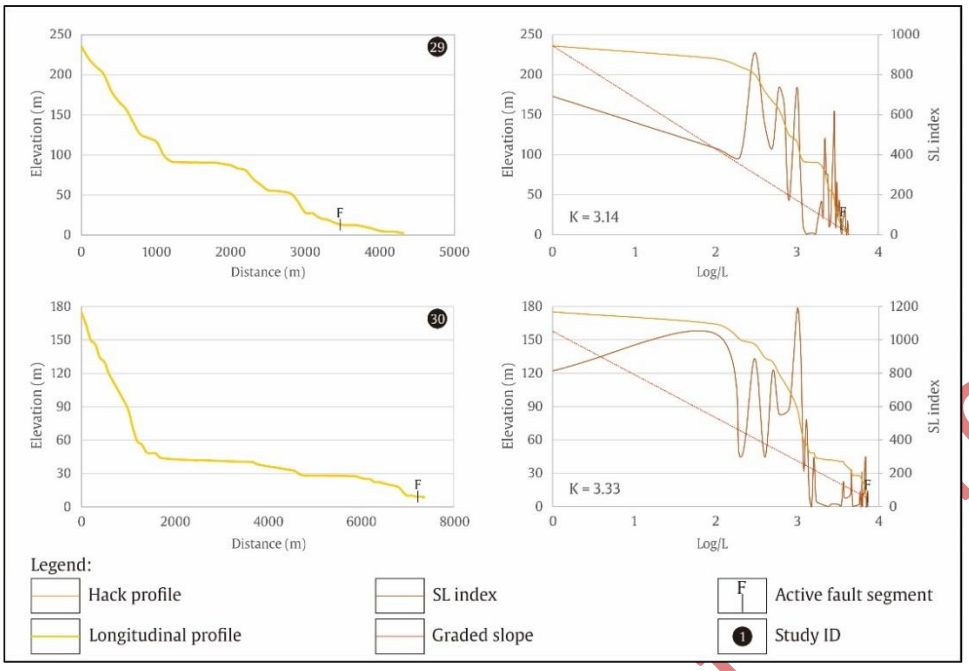

Fig. 14. Longitudinal profile, Hack profile, and SL indexes at Weleri segment.

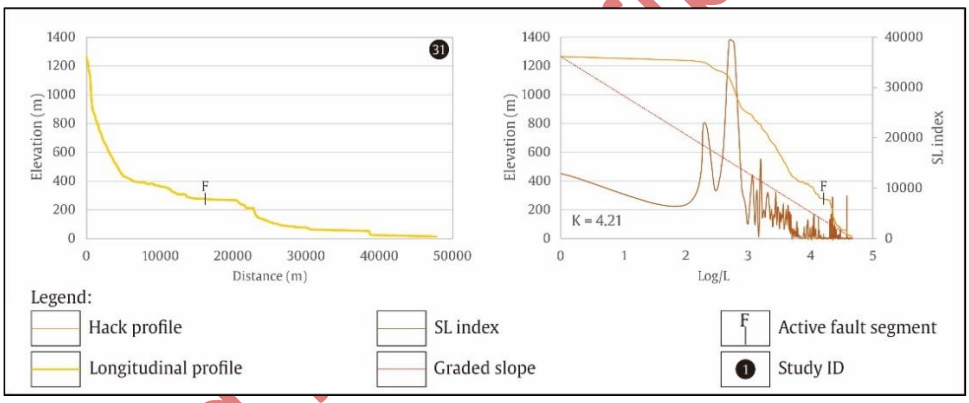

Fig. 15. Longitudinal profile, Hack profile, and SL indexes at Ungaran segment.

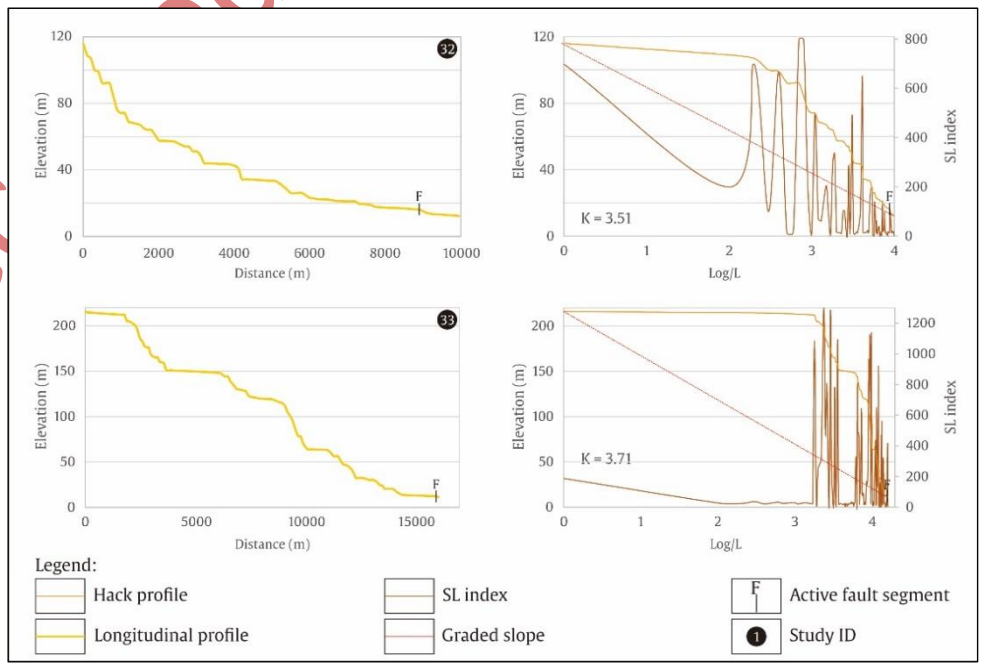

Fig. 16. Longitudinal profile, Hack profile, and SL indexes at Semarang segment.

4.2 Hypsometric Integral (HI)

The Hypsometric Integral (HI) values were calculated, and the hypsometric curve (Fig. 17) were extracted for 33 watersheds. The evolution stage of the streams can be analyzed base don the HI values and the relative shape of the hypsometric curves.

In the Cirebon-1 segment, the hypsometric curves for Ci Pakeleran to Kali Jaga exhibit two forms: concave for Ci Pakeleran, Ci Keuyeup, and Kali Pengasinan, and between S-shaped and concave for Ci Siluk and Kali Jaga. The HI values for this segment range from 0.485 to 0.506, with an average of 0.492, indicating that the watersheds in this segment are in the youthful stage.

The hypsometric curves for Ci Kanci to Ci Lambu are between concave and S-shaped, with HI values ranging from 0.484 to 0.494 and an average of 0.488. This indicates that the watersheds in this segment are also in the youthful stage.

In the Cirebon-2 segment, Ci Panundaan to Ci Jangkelok are likewise in the youthful stage. The hypsometric curves for these watersheds are concave for Ci Panundaan, Kali Kelampis, and Ci Jangkelok, while Ci Beres is between S-shaped and concave. The HI values for this segment range from 0.477 to 0.499, with an average of 0.486.

In the Brebes segment, the hypsometric curves for Kali Gurujugan to Kali Rambutan are concave, with HI values ranging from 0.417 to 0.491 and an average of 0.459, showing that these watersheds are in the youthful stage.

In the Tegal segment, the hypsometric curves for Kali Wuri-Kali Semedo have two forms, those are concave for Kali Kawung, and berween S-shaped and concave for Kali Wuri, Kali Cenang, and Kali Semedo. The HI values for this segment range from 0.467 to 0.499, with an average of 0.486. Based on this average, the watersheds in this segment are classified as being in the youthful stage.

The Pemalang segment is also classified as being in the youthful stage, based on the HI values for Kali Waluh to Kali Comal, which range from 0.472 to 0.488, with an average of 0.480. The hypsometric curves for the watersheds in this segment are concave.

In the Pekalongan segment, the hypsometric curves for Kali Paingen and Kali Sengkarang are between S-shaped and concave, with HI values ranging from 0.480 to 0.481, and an average of 0.481. This indicates that the watersheds in this segment are in the youthful stage.

The Weleri segment shows a similar pattern to the Pekalongan segment. The hypsometric curves for Kali Kadunguling and Kali Maron are between S-shaped and concave, with HI values ranging from 0.472 to 0.499 and an average of 0.485, also indicating a youthful stage.

The hypsometric curve for Kali Blorong in the Ungaran segment is concave, with an HI value of 0.476, indicating that it is in the youthful stage.

Lastly, the Semarang segment, covering Kali Loning and Kali Pakis, shows HI values ranging from 0.474 to 0.492, with an average of 0.483. The hypsometric curves for these watersheds are between S-shaped and concave, which classifies them as being in the youthful stage.

Table 2 presents the results of the analyses that have been conducted. Based on this analysis, the average values of the watersheds for each segment traversed by the streams have been recalculated.

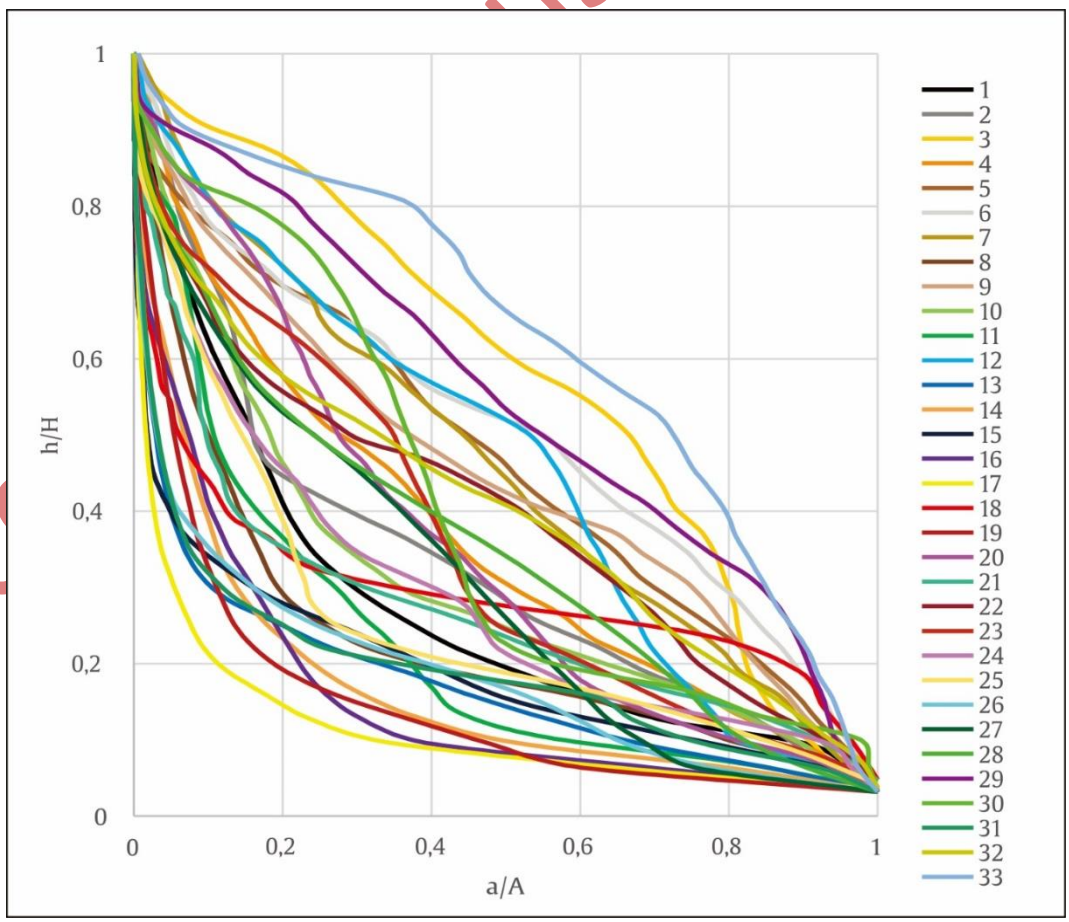

Fig. 17. Hypsometric curves of the 33 streams.

Table 2. Hypsometric integral (HI) and stream length gradient (SL) of the 33 streams in research area.

Segmen	ID	Stream name	Stream length (km)	HI	SL	K	SL/K
Cirebon-1	1	Ci Pakeleran	22.437	0.485	2825.437	3.886	726.962
Cirebon-1	2	Ci Keuyeup	8.749	0.506	196.285	3.414	57.489
Cirebon-1	3	Ci Siluk	15.042	0.488	357.691	3.693	96.849
Cirebon-1	4	Kali Pengasinan	4.732	0.486	189.391	3.047	62.145
Cirebon-1	5	Kali Jaga	8.570	0.493	274.207	3.444	79.618
Average				**0.492**	**768.602**	**3.496**	**204.641**
Cirebon	6	Ci Kanci	14.927	0.490	426.670	3.686	115.754
Cirebon	7	Kali Canggah	6.915	0.485	198.288	3.338	59.403
Cirebon	8	Ci Hambar	28.597	0.494	2920.026	3.978	734.043
Cirebon	9	Ci Juray	23.889	0.488	557.498	3.911	142.546
Cirebon	10	Ci Lambu	6.215	0.484	72.530	3.258	22.262
Average				**0.488**	**835.002**	**3.634**	**214.801**
Cirebon-2	11	Ci Panundaan	12.406	0.489	95.506	3.592	26.588
Cirebon-2	12	Ci Beres	36.546	0.499	263.451	4.075	64.650
Cirebon-2	13	Kali Kelampis	81.121	0.478	1383.986	4.449	311.078
Cirebon-2	14	Ci Jangkelok	38.660	0.477	793.435	4.130	192.115
Average				**0.486**	**634.094**	**4.061**	**148.608**
Brebes	15	Kali Gurujugan	10.693	0.417	20.727	3.535	5.863
Brebes	16	Ci Caruy	38.676	0.481	509.683	4.143	123.022
Brebes	17	Kali Babakan	36.668	0.491	818.319	4.117	198.765
Brebes	18	Kali Bogor	14.621	0.427	44.586	3.724	11.972
Brebes	19	Kali Rambutan	25.700	0.477	422.493	3.847	109.824
Average				**0.459**	**363.161**	**3.873**	**89.889**
Tegal	20	Kali Wuri	11.441	0.489	150.561	3.541	42.519
Tegal	21	Kali Kawung	8.505	0.467	108.164	3.308	32.697
Tegal	22	Kali Cenang	8.413	0.499	60.463	3.458	17.484
Tegal	23	Kali Semendo	12.050	0.489	78.618	3.526	22.296
Average				**0.486**	**99.451**	**3.458**	**28.749**
Pemalang	24	Kali Waluh	52.537	0.488	515.296	4.270	120.678
Pemalang	25	Kali Genjor	14.820	0.472	48.757	3.688	13.220
Pemalang	26	Kali Comal	73.757	0.480	2477.133	4.350	569.455
Average				**0.480**	**1013.729**	**4.102**	**234.451**
Pekalongan	27	Kali Paingen	54.858	0.481	118.973	4.261	27.921
Pekalongan	28	Kali Sengkarang	44.629	0.481	2072.529	4.200	493.459
Average				**0.481**	**1095.751**	**4.230**	**260.690**
Weleri	29	Kali Kadunguling	4.325	0.472	239.014	3.149	75.901
Weleri	30	Kali Maron	7.389	0.499	226.680	3.332	68.031
Average				**0.485**	**232.847**	**3.240**	**71.966**
Ungaran	31	Kali Blorong	47.897	0.476	1453.636	4.215	344.872
Average				**0.476**	**1453.636**	**4.215**	**344.872**
Semarang	32	Kali Loning	9.978	0.474	114.544	3.512	32.615
Semarang	33	Kali Pakis	16.077	0.492	218.911	3.714	58.942
Average				**0.483**	**166.727**	**3.613**	**45.778**

5. Discussion

Geomorphic indices are widely used to detect fault activity. Indices such as the longitudinal profile, Hypsometric Integral (HI), and SL/K value form the Cirebon-Semarang segments reveal significant differences. These variations are controlled by tectonic activity, lithological differences, and rainfall distribution. Given the relatively large research area, differences in rainfall across segments may contribute to the observed geomorphic indices. However, the primary factors influencing these indices are tectonic activity and lithology along the segments.

In terms of lithology, the Cirebon-Semarang segments exhibit distinct rock formations. In the Cirebon-1 segment, there is a combination of sedimentary and volcanic rocks, which influences the geomorphological profiles of the streams in this segment. Furthermore, the Brebes-Pemalang segments are dominnated by clastic and carbonate rocks from older formations. In these segments, the differences in rock formations are significantly distinct compared to the surrounding areas. Fault activity also plays a role in causing these lithological differences.

Based on geomorphic analysis, fault activity observed through HI and SL/K ratio values indicates that fault activity remains very strong in some segments, particularly in the Ungaran and Pekalongan segments. In these two segments, the SL/K values reach 344.872 and 260.690, respectively. These values suggest significant tectonic uplift. Additionally, the Cirebon-1 segment also shows strong activity, with a SL/K value of 204.641, indicating active tectonic processes causing uplift in that area.

The longitudinal profiles of the 33 watersheds examined along the fault segments show steep gradients, with most Hack profiles experiencing sharp declines near the main fault. The average HI values in this region range from 0.459 to 0.492, indicating that the landscape along these segments is in a youthful stage.

Geomorphic indices (HI and SL/K values) were also used to analyze fault activity segmentation. The average HI and SL/K values in the major segments show varying patterns of activity. In the Cirebon and Pemalang segments, the average HI values range from 0.488 and 0.480, while the SL/K values are 214.801 and 234.451, respectively. This data suggests that fault activity in these segments remains relatively high, with observable uplift in these areas. In the Ungaran segment, tectonic activity appears to be very strong, with a significantly high SL/K value. This indicates greater uplift in the eastern part of research area.

Thus, the results of this geomorphic analysis indicate that fault activity in the Cirebon-Semarang region remains

highly active, with stronger activity observed in the eastern and western parts compared to the central part (Table 3).

Table 3. The result of the 33 streams in research area

ID	Segments name	HIv	SLv	Kv	SLv/Kv
1-5	Cirebon-1	0.492	768.602	3.496	204.641
6-10	Cirebon	0.488	835.002	3.634	214.801
11-14	Cirebon-2	0.486	634.094	4.061	148.608
15-19	Brebes	0.459	363.161	3.873	89.889
20-23	Tegal	0.486	99.451	3.458	28.749
24-26	Pemalang	0.480	1013.729	4.102	234.451
27-28	Pekalongan	0.481	1095.751	4.230	260.690
29-30	Weleri	0.485	232.847	3.240	71.466
31	Ungaran	0.476	1453.636	4.215	344.872
32-33	Semarang	0.483	166.727	3.613	45.778

6. Conclusion

Based on the analysis conducted, it can be concluded that fault activity along the Cirebon to Semarang segments remains highly active. The HI values, generally ranging from 0.459 to 0.492, indicated that the landscape in this area is relatively young, reflecting ongoing tectonic uplift. Segments such as Ungaran, Pekalongan, and Pemalang exhibit significant uplift, with high SL/K values, particularly in the Ungaran segment, which has a SL/K value of 344.872. This activity appears to be stronger in the western and eastern parts of the research area, with greater uploft compared to the central part.

Overall, this research confirms that active tectonic processes in this region continue to play a significant role in shaping the geomorphology of the streams and landscape. This suggests that the Cirebon-Semarang segments is one of the key active tectonic features on the island of Java.

References

Achdan, A., Sudana, D., 1992. Peta geologi lembar Indramayu, Jawa. Pusat Penelitian dan Pengembangan Geologi.

Budhitrisna, T., 1986. Peta geologi lembar Tasikmalaya, Jawa Barat. Pusat Penelitian dan Pengembangan Geologi.

Chondon, W.H., Pardyanto, L., Ketner, K.B., Amin, T.C., Gafoer, S., Samodra, H., 1996. Peta geologi lembar Banjarnegara dan Pekalongan, Jawa. Pusat Penelitian dan Pengembangan Geologi.

Djuri, M., Samodra, H., Amin, T.C., Gafoer, S., 1996. Peta geologi lembar Purwokerto dan Tegal, Jawa. Pusat Penelitian dan Pengembangan Geologi.

Djuri., 1995. Peta geologi lembar Arjawinangun, Jawa. Pusat Penelitian dan Pengembangan Geologi.

Ekström, G., Nettles, M., and Dziewonski, A. M., 2012. The global CMT project 2004-2010: Centroid-moment tensors for 13,017 earthquakes, Phys. Earth Planet. Inter, 9, 200–201.

Hamilton, W, B., 1979. Tectonics of the Indonesian Region. US Govt. Print.Off.

Hamzah et al., 2013. Tectonic Geomorphology Analysis of the Baribis Fault System in the Majalengka Area and Its Surroundings. Jurnal Gunungapi & Mitigasi Bencana Geologi 5, 19-32.

Jannah, M., Astyka, P., Imam, A. S., 2024. Morphotectonic evaluation of the Baribis Kendeng faults in the Cirebon-Semarang segments and its surroundings, Central Java. Master's Thesis. Institut Teknologi Bandung.

Keller, E.A., Pinter, N., 2002. Active Tectonics: Earthquakes, Uplift, and Landscape. Prentice Hall, New Jersey, pp. 121–185.

Keller, E. A., Pinter, N., 1996. Active Tectonics Earthquake, Uplift and Landscape. Prentise Hall, Upper Saddle River, New Jersey.

Koulali, A., Susilo, S., McClusky, S., Meilano, I., Cummins, P., Tregoning, P., Lister, G., Efendi, J., Syafi'I, M.A., 2016. Crustal Strain Partitioning and the Associated Earthquake Hazard in the Eastern Sunda-Banda Arc. Geophysical Research Letters. 43(5), 1943-1949.

Marliyani, G.I., 2016. Neotectonics of Java, Indonesia: Crustal Deformation in the Overriding Plate of an Orthogonal Subduction System. Arizona State University (dissertation).

Mayer, L., 1990. Introduction to Quantitative Geomorphology, Prentice Hall, Englewood Cliffs, NJ.

Natawidjaja, D.H., Daryono, M.R., 2016. Present-day tectonics and Earthquake History of Java, Indonesia. In Proceedings GEOSEA XIV Congress and 45th IAGI Annual Convention 2016.

Pamumpuni, A., Sapiie, B., Ipranta., and Sadisun, I. A., 2022. Geomorfologi sesar aktif di Pulau Rumberpon, Papua Barat, Indonesia. Bulletin of Geology, 6, 892-900. doi: 10.5614 /bull.geol.2022.6.1.4.

Pusat Studi Gempa Nasional., 2017. Peta Sumber Daya dan Bahaya Gempa Indonesia Tahun 2017. 1, 1-400.

QGIS Development Team., 2022. QGIS Geographic Information System, retrieved from internet: https://www.qgis.org.

Silitonga, P.H., Masria, M., Suwarna, N., 1996. Peta geologi lembar Cirebon, Jawa. Pusat Penelitian dan Pengembangan Geologi.

Simandjuntak, T.O., Barber, A.J., 1996. Constrating Tectonic Styles in the Neogene Orogenic Belts of Indonesia. Geological Society, London. 106(1), 185-201.

Smyth, H.R., Hall, R., Nichols, G.J., 2008. Cenozoic Volcanic Arc History of East Java, Indonesia: the Stratigrapic Record of Eruptions on an Active Continental Margin. Geological Society of America Special Papers. 436, 199-222.

Snow, R.S., Slingerland, R.L., 1990. Stream profile adjustment to crustal warping: nonlinear results from a simple model. J. Geol. 98, 699–708. doi:10.1086/ 629434 .

Strahler, A.H., 1952. Hypsometric (area-altitude) analysis of erosional topography. Geol. Soc. Am. Bull. 63 (11), 1117–1142. doi: 10.1130/0016-7606(1952) 63 , [1117:HAAOET]2.0.CO;2.

Thanden, R.E., Sumadirdja, H., Richards, P.W., Sutisna, K., Amin, T.C., 1996. Peta geologi lembar Magelang dan

Semarang, Jawa. Pusat Penelitian dan Pengembangan Geologi.

Wheeler, D.A., 1979. The overall shape of longitudinal profiles of streams. In: Geographical Approaches to Fluvial Processes. Geo Abstracts, Norwich, pp. 241–260.

Yang, Y., Qin, X., Shi, W., Zhang, Y., Zhao, Z., 2022. Segmentation of the active Liumugao Fault, NE Tinetan Plateau as revealed by DEM-derived geomorphic indices. Geosystems and Geoenvironment.1, 1-13.